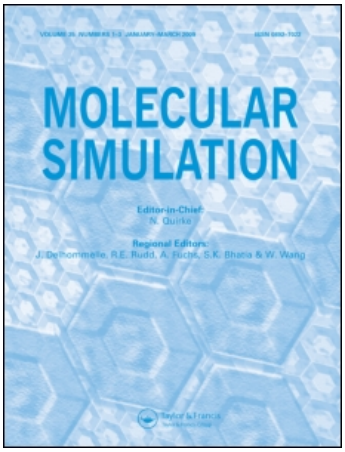

Molecular Simulation
Publication details, including instructions for authors and subscription information:
http://www.informaworld.com/smpp/title~content=t713644482

Light gas adsorption of all-silica DDR- and MFI-type zeolite: computational and experimental investigation

S. Himeno[a]; M. Takenaka[a]; S. Shimura[a]
[a] Nagaoka University of Technology, Civil and Environmental Engineering, Nagaoka, Nigara, Japan

To cite this Article Himeno, S. , Takenaka, M. and Shimura, S.(2008) 'Light gas adsorption of all-silica DDR- and MFI-type zeolite: computational and experimental investigation', Molecular Simulation, 34: 10, 1329 — 1336
To link to this Article: DOI: 10.1080/08927020802411703
URL: http://dx.doi.org/10.1080/08927020802411703

Molecular Simulation
Vol. 34, Nos. 10–15, September–December 2008, 1329–1336

Taylor & Francis
Taylor & Francis Group

Light gas adsorption of all-silica DDR- and MFI-type zeolite: computational and experimental investigation

S. Himeno*, M. Takenaka and S. Shimura

Nagaoka University of Technology, Civil and Environmental Engineering, Nagaoka, Nigara, Japan

(*Received 31 January 2008; final version received 12 August 2008*)

Grand canonical Monte Carlo simulations (GCMC) of adsorption of CO_2 and N_2 were carried out using the software Materials Studio 4.1 on all-silica DDR- and MFI-type zeolite. The simulated values of sorption capacity, isosteric heat of adsorption and Henry's constant for all-silica DDR- and MFI-type zeolite showed good agreement with experimental data. Accurate pure and binary adsorption data were measured for all-silica DDR-type zeolite crystals. Furthermore, the GCMC simulation was used to assess the adsorption properties and selectivity of CO_2/N_2 mixture gas as a function of gas phase composition and pressure. Thermodynamic properties and binary mixtures of adsorption showed good agreement with our simulation and experiments.

Keywords: adsorption equilibrium; zeolite; adsorption properties; simulation

1. Introduction

Zeolite is used for various systems because of its adsorbent with molecular sieving effect [1–9]. Many authors have reported the separation of CO_2/N_2 gases using zeolite of various types [10–16]. The results of several studies indicate that CO_2 is adsorbed strongly by zeolites, suggesting that zeolites can play a useful role in CO_2-capture technologies [17,18].

Considerable interest in DDR-type zeolite has arisen recently because of molecular sieving. Zhu et al. [2,3] determined the adsorption isotherms of ethane, propane and propene on DD3R. Our previous study measured the adsorption isotherms of CO_2 and N_2 on all-silica DDR-type (DD3R) zeolite accurately for widely various pressures and temperatures [1]. Krishna and co-workers investigated adsorption and diffusion of mixture gas in DD3R zeolite using Monte Carlo analysis and molecular dynamics [19,20].

However, the binary adsorption is not reported because the experiments are difficult. Molecular simulation methods have become an effective and complementary tool for studying zeolite sorption. Computer simulations are currently of increasing importance. Moreover, computer simulation is particularly helpful for gaining insight into structure–property relationships. They are used in conjunction with experimental techniques, over which they have the marked advantage that a wide range of conditions can be simulated, including conditions that might be difficult to achieve experimentally. Grand canonical Monte Carlo (GCMC) techniques are particularly well suited to this purpose. Given an accurate energetic and geometric model (force field) for the system of interest, the GCMC methods demonstrably provide quantitative agreement with sorption experiments results.

This paper describes the sorption properties of CO_2 and N_2 in DD3R zeolite. Furthermore, it describes the adsorption isotherms on all-silica MFI-type zeolite (silicalite): universal zeolite. In this work, the sorption of CO_2 and N_2 in DD3R was studied comparatively using the GCMC simulations. The Henry constants, isosteric heats of sorption, adsorption isotherms, sorption sites and interaction energies of guest–host relations were investigated. First, we present a molecular simulation result for DD3R zeolite of the CO_2 and N_2 adsorption isotherms and comparison with experimental data. Next, pure CO_2, N_2 and binary mixtures were predicted for use with DD3R zeolite in different temperatures, pressures and compositions using the GCMC. Additionally, we report adsorption energy measurement for pure gas and binary gas on DD3R zeolite.

2. Simulation models and methods

2.1 Models

For this study, we used structured MFI- and DDR-type zeolites to test our simulation and its all-silica-type silicalite and DD3R. Crystallographic data are available elsewhere [21]. Silicalite, an all-silica MFI framework, is a material with orthorhombic symmetry Pnma and cell parameters $a = 20.07$ Å, $b = 19.92$ Å and $c = 13.42$ Å. Silicalite has straight channels running parallel to [0 1 0] with 10-membered rings of 5.4 Å × 5.6 Å and sinusoidal channels running parallel to [1 0 0] with 10-membered

*Corresponding author. Email: himeno@vos.nagaokaut.ac.jp

ISSN 0892-7022 print/ISSN 1029-0435 online

DOI: 10.1080/08927020802411703
http://www.informaworld.com

rings of 5.1 Å × 5.5 Å. Silicalite consists of an interconnected network of 'straight' and 'zigzag' pores; these channels cross at the intersections. Actually, DD3R is an all-silica DDR-type zeolite material with orthorhombically symmetrical Pnma and cell parameters $a = 13.86$ Å, $b = 13.86$ Å and $c = 40.89$ Å [22]. The DDR topology comprises 19-hedron cavities connected through eight-ring windows of 0.36 nm × 0.44 nm across hexagonally arranged two-dimensional cage/window-type systems. It has three cage types, as shown in Figure 1: (a) DD3R zeolite structure, (b) decahedra, (c) dodecahedra and (d) 19-hedra. The 19-hedra cages are connected through eight-ring windows. The other cage types are inaccessible from the outside. For this reason, molecules cannot be inserted into these inaccessible cages during a GCMC. Dummy atoms with appropriate van der Waals' radii were introduced into the decahedra and dodecahedra to avoid introduction of adsorbates in this space for DD3R [23–26]. Figure 2 shows the framework structure and accessible volume of silicalite and DD3R.

The simulation unit cell used in this study consists of 2 × 2 × 2 unit cell. Periodic boundary conditions were used. Since the cut-off length for the non-bonding interaction of DD3R and silicalite are fixed at 6.7 and 7.6 Å, which is shorter than half the length of the unit cell, this condition is regarded as the limit of an infinitely dilute adsorbate region. The GCMC simulations at fixed temperature *T*, volume *V* and adsorbate chemical potential μ were carried out for the adsorption of pure CO_2, N_2 and mixture in zeolite. The total number of MC steps was 5,000,000, which was adequate for reaching equilibrium of the total energy and loading of the system. The zeolite lattices are rigid during simulations, with static atomic charges that are assigned by choosing $q_{si} = +0.38$ and $q_o = -0.19$. The zeolite model charges are computed using the following software: Charge Equilibration of Materials Studio. This method calculates partial charges using atomic ionisation potential, electron affinity and experiment data of the atomic radius. The CO_2 molecules are assumed linear and rigid, with bond length C—O of 1.16 Å and partial charges distributed around each molecule to reproduce a quadrupole moment experimentally. The interaction between adsorbed molecules is described using the Coulombic and Lennard-Jones terms. For CO_2 and N_2, we use the 3LJ3CB.EPM2 potential and 2LJBP model [27].

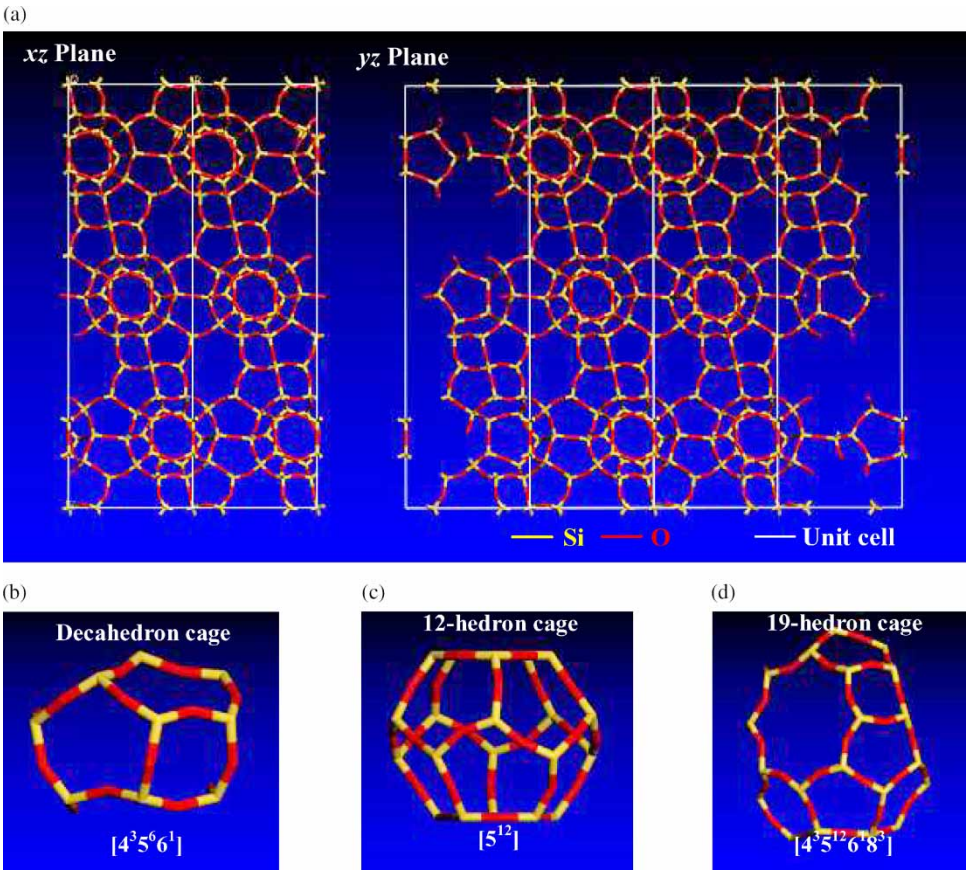

Figure 1. (a) DD3R zeolite structure, (b) decahedron cage of DD3R zeolite, (c) 12-hedron cage of DD3R zeolite and (d) 19-hedron cage of DD3R zeolite.

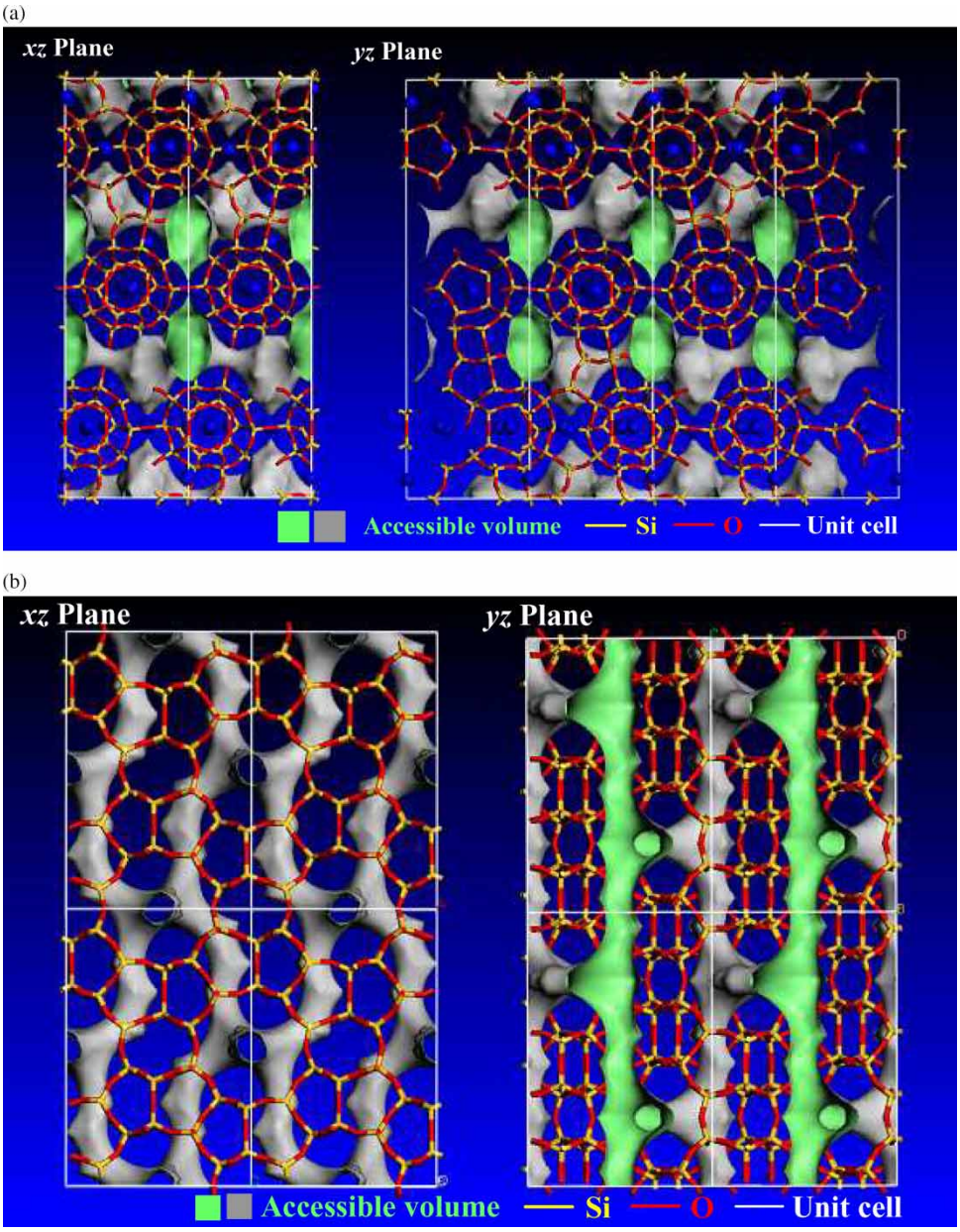

Figure 2. (a) Accessible volume on framework structure in DD3R zeolite and (b) silicalite zeolite.

2.2 Force field

We used force fields recommended by the software Cerius2 and applied the Burchart1.01–Dreiding2.21 force field to obtain a reasonable force field [28–30]. The 'Burchart1.01–Dreiding2.21' force field was developed based on the 'Burchart' and 'Dreiding' force fields. This force field incorporates four distinct interactions, including interaction within the aluminosilicate frameworks, intra- and intermolecular interactions, as well as non-bonded interaction between the framework and molecules. The 'Burchart' force field describes the framework; the 'Dreiding' force field represents the intra- and inter-molecular interactions. The cross-parameters for the framework–molecule interactions were obtained via the Lorentz–Berthelot combining rules. In the simulation, the total potential of the studied system includes bonded and non-bonded interactions. The bonding potential parameters are presented in Table 1. The non-bonded interaction incorporates van der Waals and electrostatic interactions. They are represented, respectively, as Lennard-Jones and Coulomb potentials.

3. Results and discussion

A conventional static volumetric adsorption apparatus was used to measure pure gas adsorption isotherms and

Table 1. Potential parameter for the zeolite framework and adsorbate molecules.

Atom type	ε (eV)	σ (Å)	Q (eV)
H	0.00066	3.19	−0.1200
$C_{\_CH4}$	0.00309	3.90	+0.4800
O	0.00659	3.36	−0.3256
$C_{\_CO2}$	0.00402	3.83	+0.6512
N	0.00314	3.32	0.0000
$O_{\_DD3R}$	0.00352	3.25	−0.6000
$Si_{\_DD3R}$	0.00203	3.30	+1.2000
$O_{\_MFI}$	0.00352	3.25	−0.1900
$Si_{\_MFI}$	0.00203	3.30	+0.3800

adsorption isotherms of DDR crystal at temperatures of 273–333 K and pressures up to 6 MPa as reported previously. Binary equilibrium data were measured using the volumetric flow desorption method developed at our laboratory.

For this study, binary isotherms for systems of CO_2/N_2 were measured. Absolute adsorption isotherms were computed using a GCMC calculation algorithm, as implemented in the sorption module of the Materials Studio 4.1 software suite. These simulations consisted of evaluating the average number of adsorbate molecules, whose chemical potential equals that of adsorbate molecules whose chemical potential equals that of the bulk phase for a given fugacity and temperature. To contrast our simulation against the experimental data, the fugacity and pressure were related through the relation $f = \varphi p$, where φ corresponds to the fugacity coefficient. In our case, this coefficient, which varies as function of the pressure, was evaluated through an experiment of state including the gas compressibility. All presented isotherms are absolute adsorption isotherms: experimental excess isotherms were converted into absolute isotherms [31].

3.1 Henry constant and adsorption isotherm

The selection of a proper force field is crucial for the simulation, because it is related directly to energy calculations of all molecular interactions directly. To obtain a reasonable force field, we used four force fields recommended by Materials Studio software to calculate the Henry constant and the enthalpy of adsorption of CO_2 and N_2 in DD3R and silicalite at 298 K. The results are listed in Tables 2 and 3; they suggest that the open force field

Table 2. Isosteric heat of adsorption and Henry's constants on DD3R zeolite.

	Isosteric heats (average kJ/mol)		Henry constant (mol/kg/kPa)	
Force field	CO_2	N_2	CO_2	N_2
Exp.	28.11	14.92	4.21×10^{-2}	1.50×10^{-3}
Burchart–Dreiding	28.22	14.56	4.42×10^{-2}	1.66×10^{-3}
Universal	14.15	12.61	1.82×10^{-2}	1.26×10^{-3}
Dreiding	20.69	17.01	4.45×10^{4}	8.60×10^{-3}
Universal	20.22	16.36	1.61×10^{9}	5.96×10^{-3}

Table 3. Isosteric heat of adsorption and Henry's constants on silicalite zeolite.

	Isosteric heats (average kJ/mol)		Henry constant (mol/kg/kPa)	
Force field	CO_2	N_2	CO_2	N_2
Exp.	28.50	18.09	3.85×10^{-2}	2.41×10^{-3}
Burchart–Dreiding	28.90	19.42	4.60×10^{-2}	2.50×10^{-3}
Universal	26.38	18.44	2.11×10^{-2}	1.80×10^{-3}
Dreiding	38.95	25.55	1.01	1.69×10^{-2}
Universal	35.60	23.88	3.09	1.14×10^{-2}

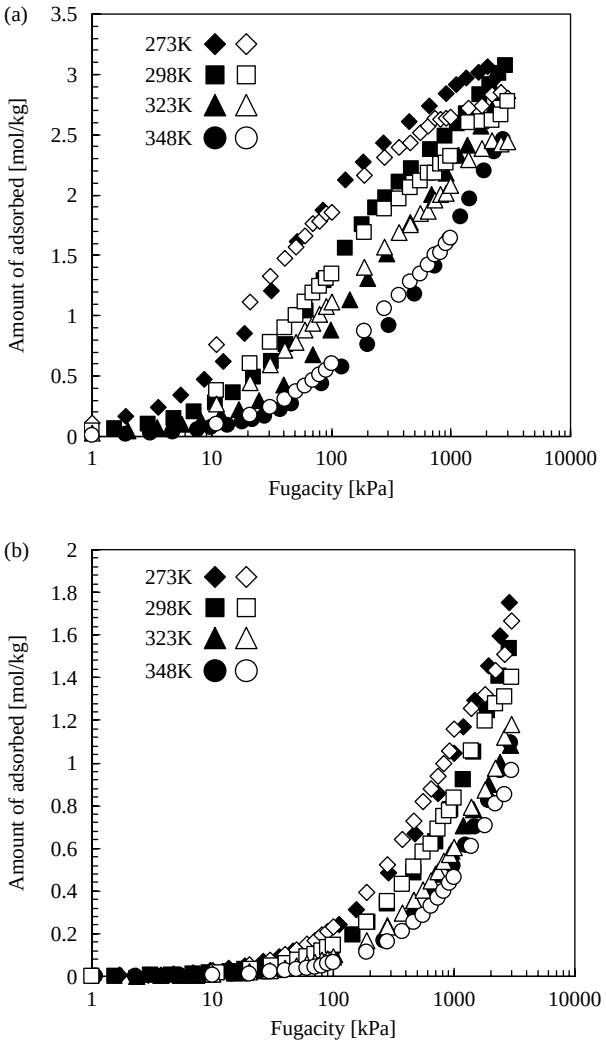

Figure 3. (a) Adsorption isotherm for CO_2 and (b) N_2 on DD3R zeolite. Open symbol, GCMC; close symbol, Expt.

'Burchart.01–Dreiding2.21' is suitable for simulations because only this force field can give a reasonable Henry constant compared with the experiments. For that reason, this force field was used in all simulations presented herein.

3.2 Adsorption isotherm

The results presented in the preceding section show that this force field is perfectly capable of reproducing experiments at both low and high loading of light gases in DD3R and silicalite. The results for the adsorption isotherms are shown in Figures 3 and 4. Several groups have determined the adsorption isotherms of small gases in silicalite. The results are comparable to those of the experiments reported by Golden and Sircar [32] and Dunne et al. [33]. Good agreement pertains between the adsorption isotherms for both CO_2 and N_2, and the

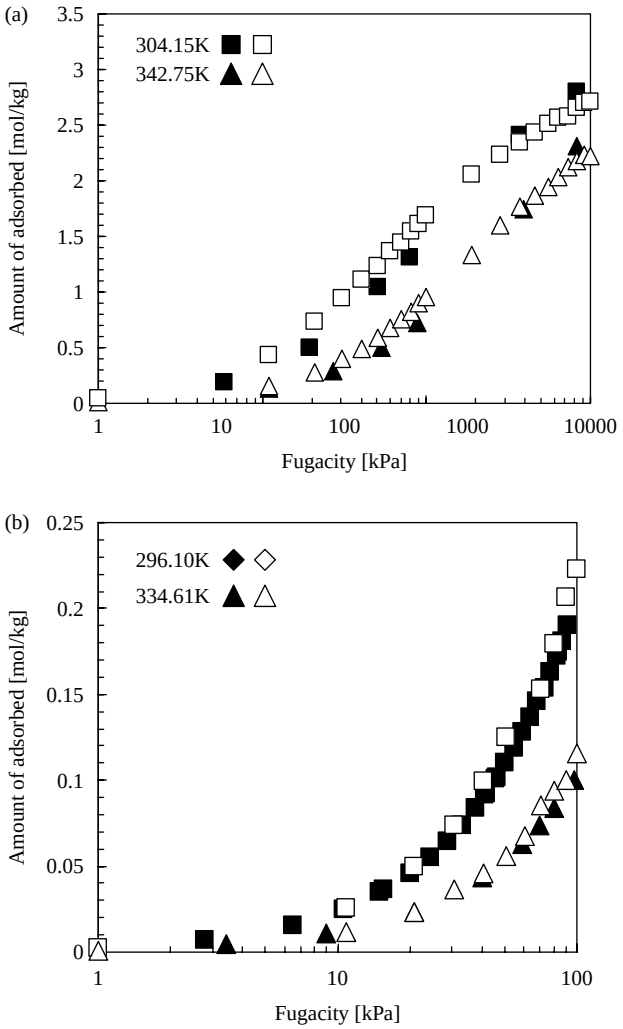

Figure 4. (a) Adsorption isotherm for CO_2 on silicalite; open symbol, GCMC; close symbol, Exp. [32]. (b) Adsorption isotherm for N_2 on silicalite; open symbol, GCMC; close symbol, Exp. [33].

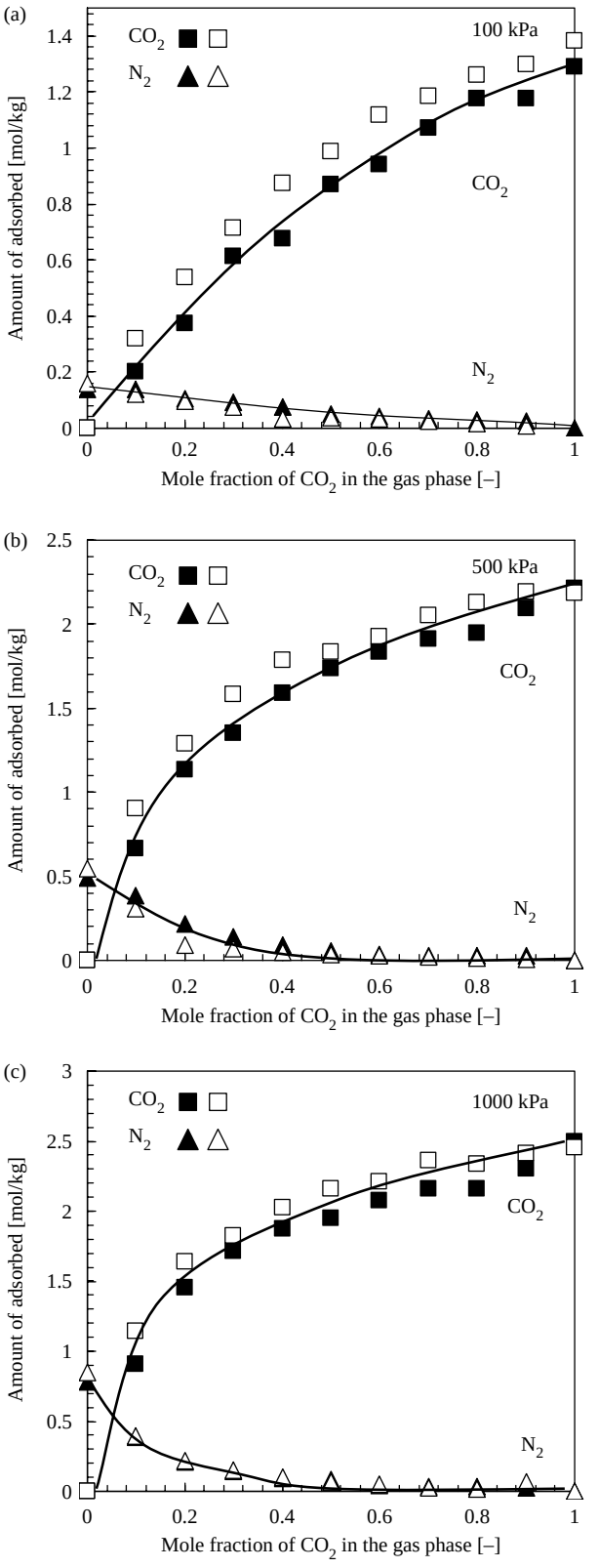

Figure 5. Binary isotherm for CO_2/N_2 gas mixtures on DD3R zeolite at 298K, at pressures of (a) 100 kPa, (b) 500 kPa and (c) 1000 kPa. Open symbol, GCMC; close symbol: Expt. The lines serve as a guide to the eye.

experimental data at all temperatures for silicalite. We compared the GCMC simulation results for pure component isotherms of CO_2 and N_2 with the experimental isotherms to verify the accuracy of the force field at higher pressures. The single-component adsorption isotherms for CO_2 and N_2 in DD3R at four temperatures (273, 298, 323 and 348 K) predicted by the GCMC are compared with our experimental measurements in Figure 3. The single-component adsorption isotherms for CO_2 and N_2 in silicalite at two temperatures (307.95 and 342.75 K, 296.10 and 334.61 K) predicted by the GCMC are shown in Figure 4, for comparison with our experimental measurements. The agreement between the GCMC simulations and experimental data is considered to be good for a wide range of pressures and temperatures.

3.3 Binary adsorption isotherm

Of great interest in separation applications is the competitive adsorption behaviour in zeolites. Simulation conditions were such that the total pressure of the mixture was held constant, whereas the mole fractions of the mixture components were varied. The results of the binary simulations can be compared with the prediction of simulation results: experimental results for CO_2/N_2 mixtures are shown in Figure 5. The mixture equilibria data were measured at temperatures of 298 K with total pressures of 0.1, 0.5 and 1.0 MPa, and with gas phase mole fractions of 0.1–0.9.

The loadings of the individual components at fractional compositions zero and one correspond to the pure component values. Simulated results for CO_2/N_2 agree well with the simulation results. Figure 6 presents a comparison of the individual amount adsorbed and selectivities as a function of total pressure in gas phase with an equimolar ratio. The adsorption selectivity of the equimolar ratio of CO_2/N_2 mixture gases of DD3R crystal was 30 at 298 K and 500 kPa. The selectivities of CO_2/N_2 (50:50) were almost unchanged.

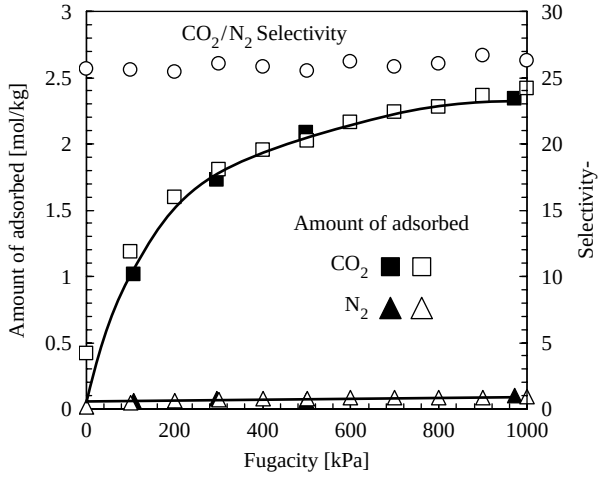

Figure 6. Binary isotherm and adsorption selectivity for CO_2/N_2 (5:5) gas mixtures on DD3R zeolite at 298 K. Open symbol, GCMC; close symbol, Expt. The lines serve as a guide to the eye.

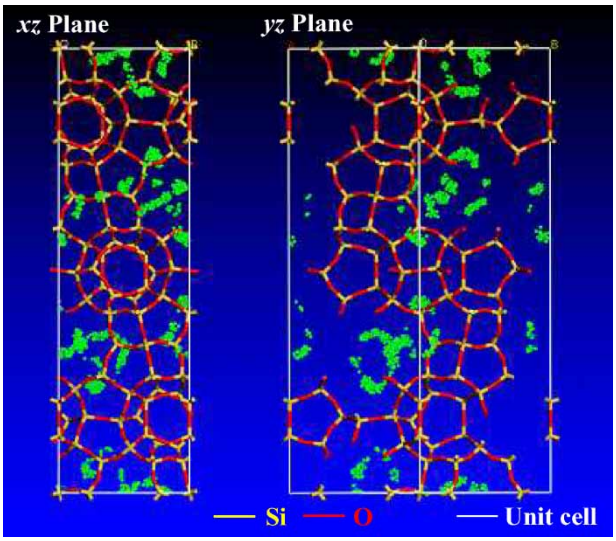

Figure 7. GCMC result for the distribution of CO_2 sorption site in DD3R zeolite framework; 298 K, 1000 kPa.

3.4 Adsorption site and interaction energy

Figures 7–9 depict adsorption sites of the molecules in the zeolite. All molecules remain in the zeolite's 19-hedron cage. All phenomena can also be presented by the sorption energy distribution of CO_2 and N_2 (Figures 10 and 11).

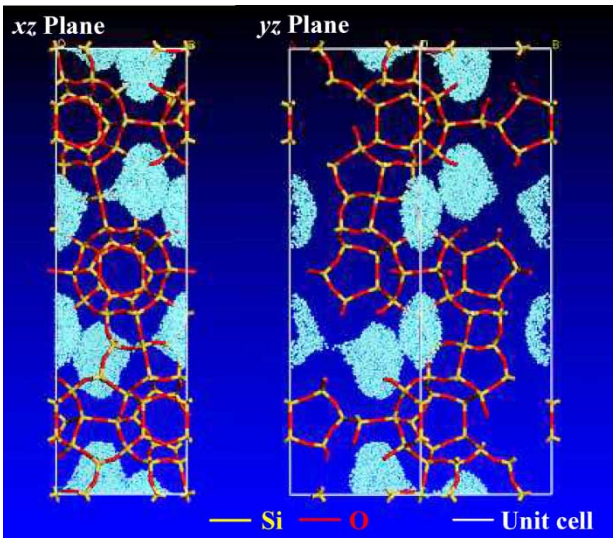

Figure 8. GCMC result for the distribution of N_2 sorption site in DD3R zeolite framework; 298 K, 1000 kPa.

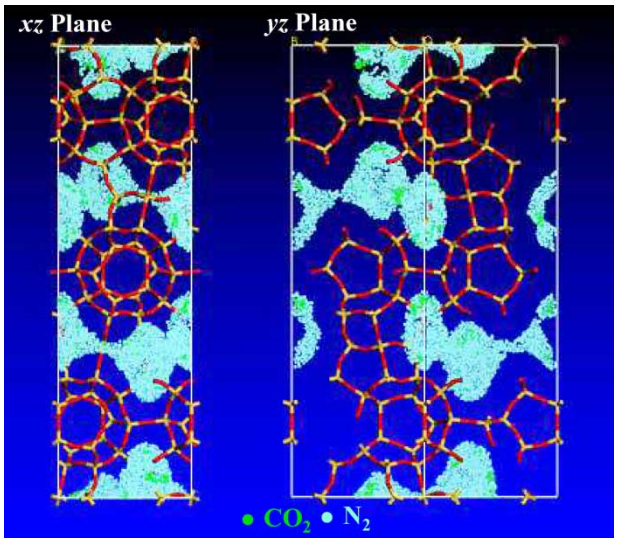

Figure 9. GCMC result for the distribution of CO_2/N_2 gas mixture sorption site in DD3R zeolite framework; 298 K, 1000 kPa.

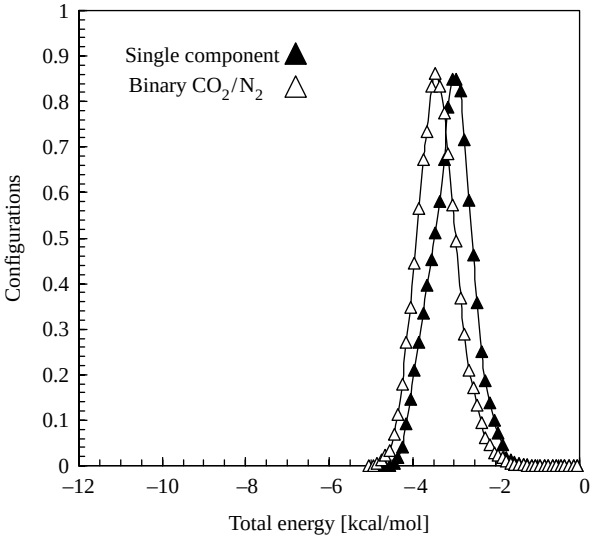

Figure 11. Distribution of total potential energy for sorption of N_2 on DD3R zeolite; 298 K, 1000 kPa.

The difference in the sorption properties of DD3R is attributed to the difference in the interaction energies between the guest molecules and the zeolite frameworks. One discrete peak for all sorbates indicates that there are many adsorption sites, one of which is the preferred site. In the case of N_2 in DD3R, however, the total energy of binary adsorption rose to the pure adsorption. This is because the interaction with the adsorbate molecule of another element was obtained because of the binary adsorption. The peak of potential energy of pure CO_2 is -6.65 kcal/mol and pure N_2 is -3.45 kcal/mol, as shown in Figures 10 and 11. And hence, it is thought that selectivity rises at CO_2 adsorption interaction if the adsorbent is strong. This means that quadrupolar CO_2 molecule is four times stronger than N_2 molecule.

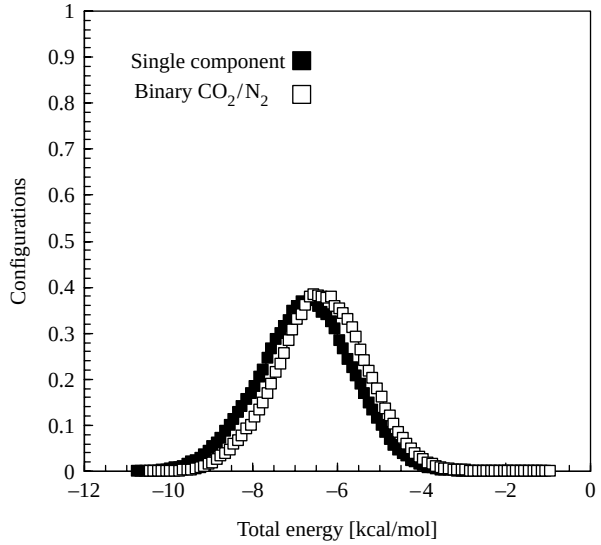

Figure 10. Distribution of total potential energy for sorption of CO_2 on DD3R zeolite; 298 K, 1000 kPa.

4. Conclusion

This paper shows that simulation can re-create experimental data of DD3R zeolite adsorption in the case of CO_2/N_2 separation. The DD3R zeolite has advantages in CO_2/N_2 separation over NaA zeolite, which has a polar character [34]. Consequently, DD3R zeolite has high potential as a CO_2/N_2 separation material. Molecular simulation is useful to analyse DD3R zeolite's applicability to flue gas separation technology. If DD3R zeolite is an effective material for CO_2 separation enrichment, DD3R zeolite can contribute to the development of new technologies that are useful as countermeasures against global warming, such as CO_2 underground storage technology.

References

[1] S. Himeno, T. Tomita, K. Suzuki, and S. Yoshida, *Characterization and selectivity for methane and carbon dioxide adsorption on the all-silica DD3R zeolite*, Micropor. Mesopor. Mater. 98 (2007), pp. 62–69.
[2] W. Zhu, F. Kapteijn, J.A. Moulijn, and J.C. Jansen, *Selective adsorption of unsaturated linear C_4 molecules on the all-silica DD3R*, Phys. Chem. Chem. Phys. 2 (2000), pp. 1773–1779.
[3] W. Zhu, F. Kapteijn, J.A. Moulijn, M.C. den Exter, and J.C. Jansen, *Shape selectivity in adsorption on the all-silica DD3R*, Langmuir 16 (2000), pp. 3322–3329.
[4] M.D. Macedonia and E.J. Maginn, *Pure and binary component sorption equilibria of light hydrocarbons in the zeolite silicalite from grand canonical Monte Carlo simulations*, Fluid Phase Equilibria 158–160 (1999), pp. 19–27.

[5] P.J.E. Harlick and F.H. Tezel, *Adsorption of carbon dioxide, methane and nitrogen: Pure and binary mixture adsorption for ZSM-5 with SiO_2/Al_2O_3 ratio of 280*, Sep. Purif. Technol. 33 (2003), pp. 199–210.

[6] M.A. Granato, T.J.H. Vlugt, and A.E. Rodrigues, *Molecular simulation of propane-propylene binary adsorption equilibrium in zeolite 13X*, Ind. Eng. Chem. Res. 46 (2007), pp. 7239–7245.

[7] H. Tournier, A. Barreau, B. Tavitian, D.L. Roux, J.-C. Moïse, J.-P. Bellat, and C. Paulin, *Adsorption equilibrium of xylene isomers and p-diethylbenzene on a prehydrated BaX zeolite*, Ind. Eng. Chem. Res. 40 (2001), pp. 5983–5990.

[8] R.S. Todd and P.A. Webley, *Macropore diffusion dusty-gas coefficient for pelletised zeolites from breakthrough experiments in the O_2/N_2 system*, Chem. Eng. Sci. 60 (2005), pp. 4593–4608.

[9] R. Babarao, Z. Hu, J. Jiang, S. Chempath, and S.I. Sandler, *Storage and separation of CO_2 and CH_4 in silicalite, C_{168} Schwarzite, and IRMOF-1: A comparative study from Monte Carlo simulation*, Langmuir 23 (2007), pp. 659–666.

[10] S. Himeno, T. Tomita, K. Suzuki, K. Nakayama, K. Yajima, and S. Yoshida, *Synthesis and permeation properties of a DDR-type zeolite membrane for separation of CO_2/CH_4 gaseous mixtures*, Ind. Eng. Chem. Res. 46 (2007), pp. 6989–6997.

[11] S. Li, J.L. Falconer, R.D. Noble, and R. Krishna, *Modeling permeation of CO_2/CH_4, CO_2/N_2, and N_2/CH_4 mixtures across SAPO-34 membrane with the Maxwell-Stefan equations*, Ind. Eng. Chem. Res. 46 (2007), pp. 3904–3911.

[12] Y. Ohta, H. Takaba, and S. Nakao, *A combinatorial dynamic Monte Carlo approach to finding a suitable zeolite membrane structure for CO_2/N_2 separation*, Micropor. Mesopor. Mater. 101 (2007), pp. 319–323.

[13] K. Makrodimitris, G.K. Papadopoulos, and D.N. Theodorou, *Prediction of permeation properties of CO_2 and N_2 through silicalite via molecular simulations*, J. Phys. Chem. B 105 (2001), pp. 777–788.

[14] X. Gu, J. Dong, and T.M. Nenoff, *Synthesis of defect-free FAU-type zeolite membranes and separation for dry and moist CO_2/N_2 mixtures*, Ind. Eng. Chem. Res. 44 (2005), pp. 937–944.

[15] A. Goj, D.S. Sholl, E.D. Akten, and D. Kohen, *Atomistic simulations of CO_2 and N_2 adsorption in silica zeolites: The impact of pore size and shape*, J. Phys. Chem. B 106 (2002), pp. 8367–8375.

[16] P. Li and F.H. Tezel, *Equilibrium and kinetic analysis of CO_2-N_2 adsorption separation by concentration pulse chromatography*, J. Colloid Interf. Sci. 313 (2007), pp. 12–17.

[17] S. Li, J.L. Falconer, R.D. Noble, and R. Krishna, *Modeling permeation of CO_2/CH_4, CO_2/N_2, and N_2/CH_4 mixtures across SAPO-34 membrane with the Max well-Stefan equations*, Ind. Eng. Chem. Res. 46 (2007), pp. 3904–3911.

[18] R.V. Siriwardane, M.-S. Shen, E.P. Fisher, and J.A. Poston, *Adsorption of CO_2 on molecular sieves and activated carbon*, Energy Fuels 15 (2001), pp. 279–284.

[19] R. Krishna, J.M. van Baten, E. García-Pérez, and S. Calero, *Diffusion of CH_4 and CO_2 in MFI, CHA and DDR zeolites*, Chem. Phys. Lett. 429 (2006), pp. 219–224.

[20] R. Krishna and J.M. van Baten, *Influence of segregated adsorption on mixture diffusion in DDR zeolite*, Chem. Phys. Lett. 446 (2007), pp. 344–349.

[21] Ch. Baerlocher, W.M. Meier, and D.H. Olson, *Atlas of Zeolite Framework Types*, Elsevier, Amsterdam, 2002.

[22] H. Gies, *Crystal structure of deca-dodecasil 3R, the missing link between zeolites and clathrasils*, Z. Kristallogr. 175 (1986), pp. 93–104.

[23] G. Maurin, Ph. Llewellyn, Th. Poyet, and B. Kuchta, *Influence of extra-framework cations on the adsorption properties of X-Faujasite systems: Microcalorimetry and molecular simulations*, J. Phys. Chem. B 109 (2005), pp. 125–129.

[24] G. Maurin, P.L. Llewellyn, and R.G. Bell, *Adsorption mechanism of carbon dioxide in faujasites: Grand canonical Monte Carlo simulations and microcalorimetry measurements*, J. Phys. Chem. B 109 (2005), pp. 16084–16091.

[25] G. Maurin, R. Bell, B. Kuchta, T. Poyet, and P. Llewellyn, *Adsorption of non polar and quadrupolar gases in siliceous faujasite: Molecular simulations and experiments*, Adsorption 11 (2005), pp. 331–336.

[26] G. Maurin, S. Bourrelly, P.L. Llewellyn, and R. Bell, *Simulation of the adsorption properties of CH4 in faujasites up to high pressure: Comparison with microcalorimetry*, Micropor. Mesopor. Mater. 89 (2006), pp. 96–102.

[27] K. Makrodimitris, G.K. Papadopoulos, and D.N. Theodorou, *Prediction of permeation properties of CO_2 and N_2 through silicalite via molecular simulations*, J. Phys. Chem. B 105 (2001), pp. 777–788.

[28] E. Klemm, J. Wang, and G. Emig, *A comparative study of the sorption of benzene and phenol in silicalite, HAlZSM-5 and NaAlZSM-5 by computer simulation*, Micropor. Mesopor. Mater. 26 (1998), pp. 11–21.

[29] X. Chen, S. Huang, D. Cao, and W. Wang, *Optimal feed ratio of benzene–propylene binary mixtures for alkylation in ZSM-5 by molecular simulation*, Fluid Phase Equilibria 260 (2007), pp. 146–152.

[30] D. Martin and M. Guisnet, *A new automated molecular modeling method to locate coke and to follow its growth inside zeolite: Application to the coke formed during the transformation of toluene on H-MFI*, J. Catalysis 188 (1999), pp. 346–352.

[31] F. Dreisbach, R. Staudt, and J.U. Keller, *High pressure adsorption data of methane, nitrogen, carbon dioxide and their binary and ternary mixtures on activated carbon*, Adsorption 5 (1999), pp. 215–227.

[32] T.C. Golden and S. Sircar, *Gas adsorption on silicalite*, J. Colloid. Interf. Sci. 162 (1994), pp. 182–188.

[33] J.A. Dunne, R. Mariwala, M. Rao, S. Sircar, R.J. Gorte, and A.L. Myers, *Calorimetric heats of adsorption and adsorption isotherms. 1. O_2, N_2, Ar, CO_2, CH_4, C_2H_6, and SF_6 on silicalite*, Langmuir 12 (1996), pp. 5888–5895.

[34] Z. Zhou, J. Yang, Y. Zhang, L. Chang, W. Sun, and J. Wang, *NaA zeolite/carbon nanocomposite thin films with high permeance for CO_2/N_2 separation*, Sep. Purif. Technol. 55 (2007), pp. 392–395.